

A practical green synthesis method of Ag NPs using rosy periwinkle plant leaves for solar panel coating

Priya Palanichamy^{a,*}, Rajesh Krishnasamy^a, Ulaganathan Meenakshi Sundaram^b, Senthil Muthu Kumar Thiagamani^{c,i,**}, R.A Ilyas^{d,e,f,g}, Ahmed M. Hassan^h

^a Department of Electrical and Electronics Engineering, Kalasalingam Academy of Research & Education, Anand Nagar, Krishnan Koil 626126, Tamil Nadu, India

^b Department of Electrical and Electronics Engineering, P.S.R Engineering College, Sivakasi 626140, Tamil Nadu, India

^c Department of Mechanical Engineering, Kalasalingam Academy of Research & Education, Anand Nagar, Krishnan Koil 626126, Tamil Nadu, India

^d Department of Chemical Engineering, Faculty of Chemical and Energy Engineering, Universiti Teknologi Malaysia, 81310 UTM, Johor, Malaysia

^e Centre for Advanced Composite Materials, Universiti Teknologi Malaysia (UTM), Johor Bahru 81310, Malaysia

^f Institute of Tropical Forest and Forest Products (INTROP), Universiti Putra Malaysia, 43400 UPM Serdang, Selangor, Malaysia

^g Centre of Excellence for Biomass Utilization, Universiti Malaysia Perlis, 02600, Arau, Perlis, Malaysia

^h Faculty of Engineering, Future University in Egypt, 11835 Cairo, Egypt

ⁱ Department of Mechanical Engineering, INTI International University, Persiaran Perdana BBN, Putra Nilai, 71800 Nilai, Negeri Sembilan, Malaysia

ARTICLE INFO

Keywords:

Green synthesis
Silver nanoparticles
Coating
Solar panel

ABSTRACT

Coated silver nanoparticles (Ag NPs) are currently receiving interest because of their numerous uses in various fields of electronics, antimicrobials, manufacturing sectors, optical science, and pharmaceuticals. Among others, it gained significant attention in the power electronic system. The goal of the proposed study is to use a cost-effective coating material for solar panels; to accomplish this, silver nanoparticles were synthesized from the leaves of the *Rosy Periwinkle* plants. Green synthesis and characterization, such as Ultraviolet Visible Spectrometer (UV-Vis) analysis, Scanning Electron Microscopy (SEM), Energy Dispersive X-ray Spectroscopy (EDX), and Fourier Transform Infrared Spectroscopy (FTIR), were carried out after the silver nanoparticles have been collected prior coating. As a consequence, the effectiveness is determined based on the conductivity test, and the resulting Ag NPs are then applied to the c-si layer of the solar panel. Additionally, a modelling and experimental analysis are performed in this study to ascertain the suggested framework's ability to measure energy before and after coating panels with Ag NPs. Specifically, the Voltage Current (VI) and Power Voltage (PV) characteristics were validated in this study for analyzing the effectiveness and the obtained results revealed that the coating of green synthesized Ag NPs generated 2 % more power than the reference solar panel under the same conditions. Further, hardware testing and simulation were both used to confirm the outcomes and effectiveness of the suggested method. The open circuit voltage (V_{oc}), short circuit current (I_{sc}), maximum peak voltage (V_{mp}), maximum peak current (I_{mp}), and efficiency are taken into account when assessing how well the suggested system performs at tracking. Moreover, the current density characteristics were evaluated with respect to various irradiation conditions for both the typical solar as well as Ag NPs coated panels. From the observation, it is noted that the

* Corresponding author.

** Corresponding author.

E-mail addresses: priyap1805harish@gmail.com (P. Palanichamy), k.rajesh@klu.ac.in (R. Krishnasamy), tsmkumar@klu.ac.in (S.M.K. Thiagamani), ahmadilyas@utm.my (R.A Ilyas), ahmed.hassan.res@fue.edu.eg (A.M. Hassan).

<https://doi.org/10.1016/j.heliyon.2023.e22893>

Received 27 July 2023; Received in revised form 11 October 2023; Accepted 22 November 2023

Available online 27 November 2023

2405-8440/© 2023 Published by Elsevier Ltd.

This is an open access article under the CC BY-NC-ND license

(<http://creativecommons.org/licenses/by-nc-nd/4.0/>).

efficiency level of coated panel was improved up to 19.20 %, 18 %, and 17.20 % for the irradiations of 200 W/m², 500 W/m², and 1000 W/m² respectively.

1. Introduction

Acid rain and global warming are two severe issues that are brought on by traditional energy sources that produce energy by burning of fossil fuels. Therefore, green and renewable energy technologies have drawn mounting interest over the recent times. Since the sun is the only every day energy source that can be effectively used for the production of electricity, increasing the efficiency of solar panels has drawn the attention of many researchers. However, due to the diffraction at the air/glass contact and the buildup of

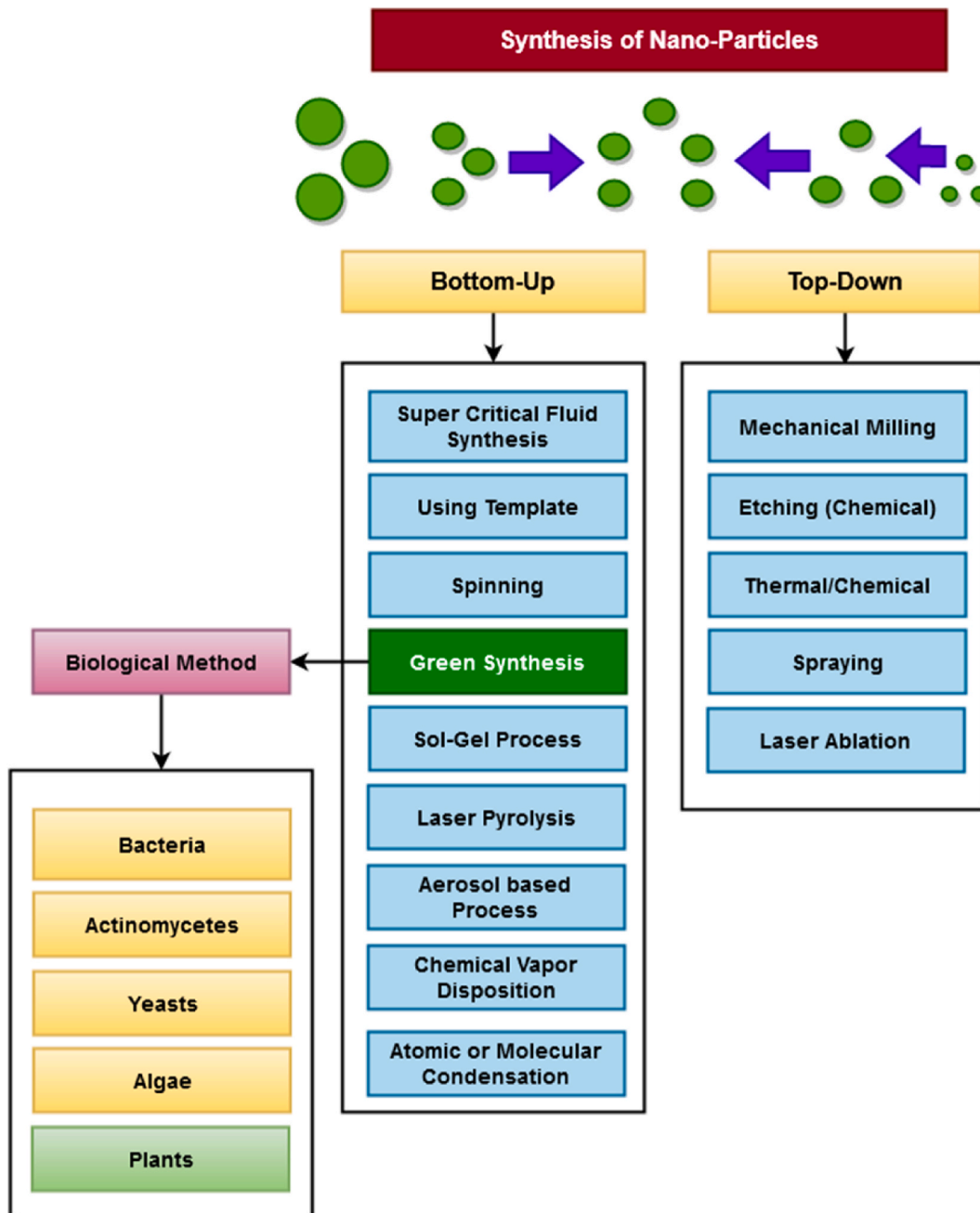


Fig. 1. Synthesis of nano-particles.

dust on the solar modules, a considerable portion of the resulting solar energy is being thrown away. Therefore, versatile thin sheets or coatings are now being used to improve the surface morphology and attributes of the solar panel materials in an effort to increase the energy transmittance, self-cleaning, and anti-reflection capabilities of the coated solar panels. Solar panel coatings have been made using a variety of materials and techniques, including surfaces that are superhydrophobic, super hydrophilic, and photoactive. Therefore, the solar panels must be coated with functional materials in order to improve the photo voltaic (PV) array performance.

Recently there is a mounting interest among the researchers on nanoparticles (NPs) because of their high ratio of surface to volume [1,2]. Silver nanoparticles (Ag NPs) can be synthesized in a variety of methods, including biologically, chemically, and organically. Since silver holds wide-spectrum of antibacterial properties, it has been used as medicine for more than 2000 years [3–6]. Silver exhibits inhibitory activity against microbes in a variety of ways. Silver-based products are inexpensive and less likely to lead to the development of antibiotic resistance [7–9]. Typically, the different types of sources such as plants, bacteria, fungi, and bio-polymers are used for the synthesis of silver nanoparticles, in which the functional components of several plant extract constituents interact electrostatically with Ag + [10]. Among others, the silver nano-particles are very essential, due to their chemical and bio-logical parameters. The hazardous chemicals used during synthesis results in unfavorable residues. Hence, there is a growing demand for developing sustainable methods for green synthesis of NPs. As a result, the research of green synthesis of Ag-NPs is progressing as a crucial area of nanotechnology, where using biological substances including plant extracts or microbes [11], or both to produce NPs could replace physical and chemical reactions in an ecologically sustainable manner. The manufacturing cost of solar panel persists to be too high when contrasted to the energy generated by fossil fuels, despite excellent research in traditional silicon and flexible film-based solar energy cells in the field of electronics, science and medicine [12]. Two basic methodologies can be used to group the endeavors that have been done in recent decades. The first one was made possible by employing wafers of silicon or films that had been deposited thinner. The other method involves creating alternative solar cells at minimal cost while maintaining a high level of overall performance.

Bouafia et al. [13] investigated about the synthesis, properties and applications of Ag NPs, with its bottom-up and top-down approaches. The synthesis of nano particles is represented below in Fig. 1. Moreover, the study indicates that among other synthesis approaches, the green synthesis from plant extract is one of the most effective methods, because it has less biosecurity risks. Different reaction parameters, such as solvent and humidity are important in green synthesis techniques that rely on biological reducing substances.

Poudel et al. [14] conducted a critical review to investigate the potential applications of Ag NPs with the green synthesis methods. The physio chemical characteristics of green synthesized Ag NPs are unique and size-dependent. Additionally, they display optical characteristics such as Surface-Enhanced Raman scattering (SERS), extensive visible and far-infrared light absorption, and a reduction in optical spectrum during surface plasma dissemination. Additionally, these particles exhibit good catalytic and biological properties, high electric and thermal conductivity, and substantial responsiveness. Castillo et al. [15] investigated some of the green synthesis methods for extracting the gold and silver nano particles. The initial step in separating plant metabolites from the basic materials is to use extraction technologies. Since these factors affect the quality of an extract, several fundamental criteria must be taken into account when conducting an extraction process.

Singh et al. [16] implemented a nano-particle based anti-reflection mechanism for coating solar panels with better performance. The main purpose of this work is to effectively minimize the reflection loss of surface with the use of anti-reflection coating mechanism. Similarly, Chugh et al. [17] conducted a detailed investigation on the different types of factors used for nano-particle synthesis. The study revealed that the biological method is one of the most preferable and suitable models for synthesis. Tabrizi et al. [18] utilized a plasmonic Ag NPs for coating solar cells in order to improve efficiency. Moreover, the authors investigated the effect of incorporation of plasmonic nano-structures on the harvesting of light in the active layer. They found that the light absorption property was highly improved by performing coupling between the plasmonic and photonic modes. Ye et al. [19] developed a new electrospun nano-fibrous membrane structure, for ultra-violet distillation. In this work, the silver particles are integrated with the nano-fibrous membranes with the use of electrospinning technique. Shashanka et al. [20] coated ZnO nano-particles on the solar cells to investigate the dye-sensitized parameters such as efficiency, fill factor, current density, short circuit and open circuit voltage. In addition, the structural evaluation, microscopy analysis, and optical characterization analysis have been performed to assess the outcomes of the suggested synthesis model.

From the literature review it is clear that there are several similar works on the green synthesis of Ag NPs, however, the usage of the

Table 1
Different types of plant leaves used for obtaining silver nano-particles.

Name of the Plant	Size (nm)	Shape	Properties	Ref
<i>Skimmialaureola</i>	40	Spherical	Antibacterial Property	[28]
<i>Mimusopselengi</i>	55–83	Spherical	Antibacterial Properties against multi-drug resistant clinical isolates	[29]
<i>Polyalthia longifolia</i>	10–40	Spherical	<i>In vitro</i> antifungal activity against phytopathogen	[30]
<i>Hibiscus sabdariffa</i>	28	Spherical	Effective Cytotoxicity	[31]
<i>Persicaria hydropiper</i>	32–77	Oval	Catalytic activity against multidrug-resistant bacteria	[32]
<i>Ocimum sanctum</i>	10–50	Spherical	Bactericidal activity	[33]
<i>Zataria Multiflora</i>	30	Pentagonal	Apoptosis in Hela Cells	[34]
<i>Allium cepa</i>	33	Spherical	Effective anti-bacterial activity	[35]
<i>Catharanthus roseus</i>	35–55	Spherical	Larvicidal effect	[36]
<i>Rosy Periwinkle</i>	35–55	Spherical	Larvicidal effect	Current Study

abundantly available *Rosy Periwinkle* as a precursor for the synthesis of Ag NPs haven't been explored till date. Furthermore, all the above-mentioned research works were related to the synthesis of NPs targeting various biological applications such as anti-bacterial, anti-fungal and cytotoxicity etc. Whereas, the novelty of the present work lies in the applicability on the solar panels. The unique characteristics of the proposed method are simple to implement, cost effective, and ensured efficiency.

2. Materials and methods

2.1. Materials

Several plant leaves were used for the synthesis of Ag NPs. Table 1 shows the various plant sources used for the synthesis of Ag NPs compared with *Rosy Periwinkle* leaves. To carry out the research work leaves of the *Rosy Periwinkle* plant were collected from a garden in Srivilliputhur, Tamil Nadu, India. Silver Nitrate ($AgNO_3$) was supplied by Sigma Aldrich, Mumbai. Ethanol was procured from Ganapathy Scientific Equipment, Srivilliputhur.

2.2. Methods

2.2.1. Synthesis of Ag NPs

Fig. 2 shows the methodology adopted in this research work. The methodology involves the collection of *Rosy Periwinkle* leaves and the extract is obtained from the leaves. To make plant leaf extracts for testing, 15 g of dried leaves were sliced in to small pieces and

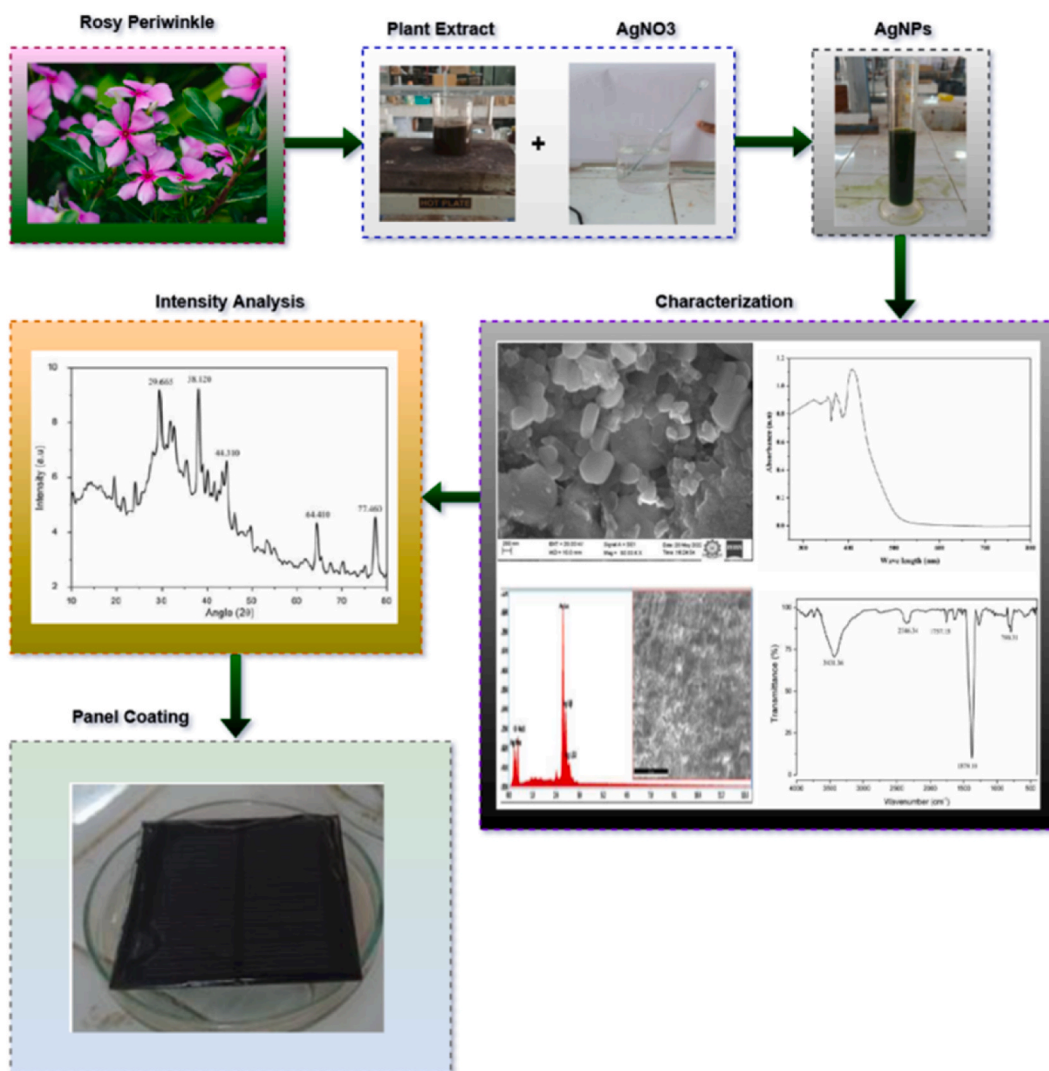


Fig. 2. Methodology adopted in the research work.

were cleaned using deionized water. The cleaned leaves were then dried and immersed in a conical vessel containing ethanol. The mixture was continuously stirred using a magnetic stirrer and heated up to 80 °C for 30 min before being filtered with the use of filter paper. Then, the necessary amount (4.2 g) of diluted AgNO₃ solution was added to 9 ml of the leaf extracts. The combination was now allowed to remain at ambient temperature overnight so that the ethanol solution gets evaporated and the Ag NPs are separated. Within 30 min of being combined with the silver ion complex solution, the leaf extract began to transform from brown to a dark brown color. The distinctive color fluctuation may be caused by the outermost plasmon resonance being excited in metal NPs, which is a sign that Ag NPs have formed. The surface plasmon resonance (SPR), which is directly tied to these particles' intriguing optical characteristics and which is greatly influenced by the shape of the samples, plays an important role in SPR. The schematic of the synthesis of Ag NPs from *Rosy Periwinkle* plant is depicted in Fig. 3.

2.2.2. Characterization

The synthesized Ag NPs were characterized by the following techniques. The UV–visible spectra were measured using a Shimadzu UV–Vis Spectrometer (UV-1800). The morphology of the Ag NPs was analyzed using a Scanning Electron Microscope (EVO18, CARL ZEISS) at a magnification of 50 K and an accelerated voltage of 20 kV. The FTIR spectra of the Ag NPs was recorded using a Fourier Transform Infrared Spectrophotometer (IR Tracer 100) in the wavelength ranging from 500 to 4000 cm⁻¹ under the reflection mode. The X-ray diffractograms of the Ag NPs are recorded in the range of 10 ° to 80 ° with the scan rate of 4 % using an X-ray diffractometer (D8 Advance ECO). The conductance was been measured using a conductivity meter (Systronics, Model 306) having standard of 0.01 NKCl. Then, the proper coating is performed in the layers of solar panel for maximum current extraction. Finally, both the simulation and real time analysis are carried out to assess the IV and PV characteristics of the solar panel. To evaluate the performance through simulation a MATLAB software tool was used to simulate the effects of coatings in solar panel. A Flash tester model (Sun Eye Series 720) was used to evaluate the effectiveness and performance of solar panels. By exposing the panels to a short burst of light that mimics sunshine, it analyses the electrical properties of the panels. Important factors including the panel's maximum power output, open-

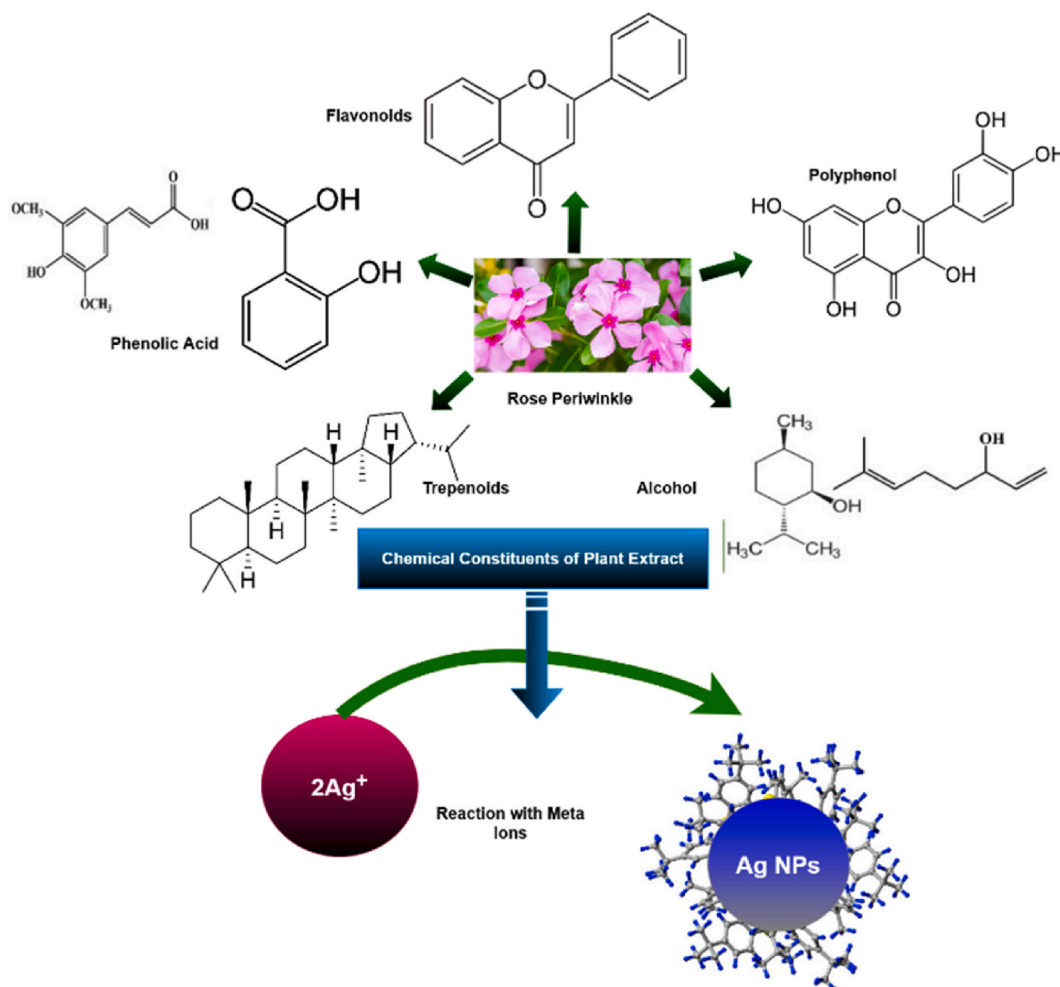


Fig. 3. Synthesis of Ag NPs from *Rosy Periwinkle* plant leaves.

circuit voltage, short-circuit current, and overall efficiency are all determined by this test.

2.2.3. Coating of Ag NPs on the solar panels

The Ag NPs are coated on the layer of the solar panel as shown in Fig. 4. In this study, the solar cell is fabricated with the use of c-Si, where a 5 nm thin coating of SiO₂ serves as a dielectric spacer between the single, spherical Ag NPs with a diameter of around 10 nm that make up the computational space and c-silicon layer. The Ag NPs were coated on the silicon semiconducting solar panels with a thickness of 300 μm using thick monocrystalline polished wafers. Using the screen-printing method, the Ag NPs was shielded on the glassy surface of the solar panels. The solar panels have been doped with Ag NPs ions, enhancing the characteristic features of the solar panels. It is to be noted that the concentration of the silver doping is directly proportional to the efficiency and accuracy of the solar panel. Investigation of the surface plasmon resonance of the Ag NPs using UV–visible spectroscopy was carried out in this work. It is to be noted that the spatial restriction of the near-field distribution happens when the posterior region of the nanoparticles receives very little energy. The plasmonic dissemination of the p-n junction solar cell arrangement with silver nanoparticles is shown in Fig. 4. Electrodes in the cell independently capture holes and electrons in a standard form of solar cell with a p-n junction. An increase in sunlight scattering is observed when the absorbing layer reflects and scatters plasmons, which results in a higher yield of the sunlight interaction inside the absorbing layer. To complete the cell arrangement with precise approximation, the restricted excitation of plasmons and the polaritons of surface the plasmons will aid in providing excitons. Moreover, the Ag nanoparticles ingrained silicon solar cells perform much better due to lower silicon substrates absorption and higher layer sunlight absorption. For validation and assessment, the IV and PV characteristics before and after panel coating are evaluated during simulation analysis and experimentation.

3. Results and discussion

3.1. Ultraviolet–visible spectrometer analysis

Fig. 5 shows the UV–Vis spectrum of Ag NPs obtained from the *Rosy Periwinkle* leaf extract. An absorption peak was observed at around 408 nm in the UV–visible spectrum of the solution. Like silver, the conduction and valence bands of metal nanoparticles are very close together, allowing electrons to move through them freely. Due to the mutual vibration of the electrons in the metal nanoparticles in resonance with a light wave, these free electrons produce a surface plasmon resonance (SPR) absorption band. The appearance of the peaks revealed the properties of Ag NPs surface plasmon resonance. Biosynthesized Ag NPs exhibit a broad spectrum because of their size and shape, resulting in an absorption peak SPR in the visible range at 408 nm.

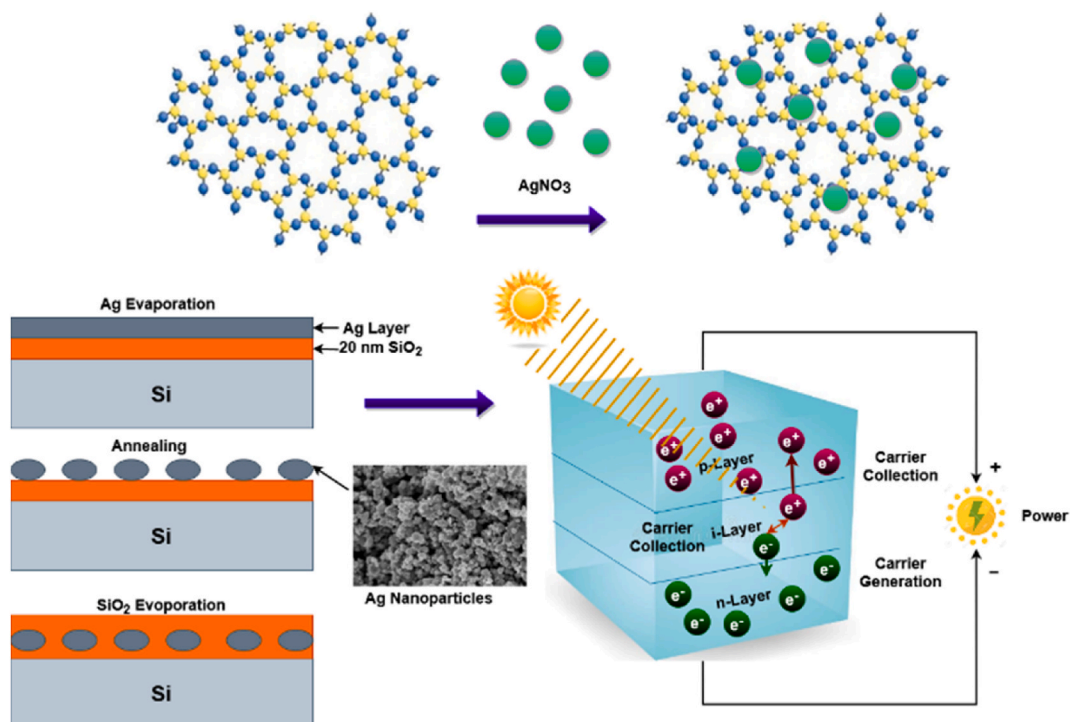


Fig. 4. Coating of Ag NPs on the solar panel.

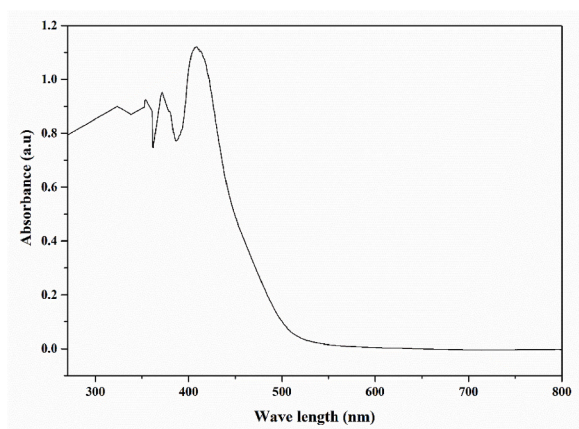


Fig. 5. UV-Vis spectra of Ag NPs.

3.2. Scanning electron microscope and Energy Dispersive X-ray spectroscopy

Using a scanning electron microscope, the surface morphology of the Ag NPs was examined. The shape of the Ag NPs was mostly found to be in spherical shape as seen in Fig. 6. Further few particles were found to agglomerated in to larger particles with unclear morphology. This aggregation could be brought on by the presence of later metabolites in the leaf extracts. The formation of Ag NPs was confirmed by an EDX spectra. The elemental profile of the Ag NPs is shown in Fig. 7. EDX was also used to identify the composition of the elements in the nanoparticles. The silver particles are homogenously presented in the synthesized nano-material, and we have tested it for multiple areas. For instance, the sample obtained results for area 1 and area 2 are given in Table 2 (a) and (b). Moreover, the findings indicate that nearly 71 % silver particles are presented in the material we taken for study.

The silver content of the synthesized product was well purified and had a significant amount of silver, as shown by the EDX mapping, which revealed that 71 % of the nanoparticles contained silver, and remaining 29 % are oxygen and carbon. Weak signals from oxygen and a strong, sharp signal in the 3–5 keV range indicate the presence of silver in the sample. The proteins, enzymes, and saccharides in the *Rosy Periwinkle* leaf extract generated weak oxygen signals.

3.3. Fourier transform infrared analysis (FTIR)

FTIR measurements were conducted to identify the functional groups present in *Rosy Periwinkle* leaf extract responsible for reducing Ag ions [21]. The reduction and capping of Ag NPs were accomplished by biomolecules found in the leaf extract. FTIR spectrum of prepared Ag NPs is shown in Fig. 8. The stretching band at 3431 cm^{-1} corresponds to O–H vibration. Two characteristic stretching bands at 2734 and 2355 cm^{-1} arise from O–H stretch from carboxylic acids [22,23]. Two peaks at 1636 and 1514 cm^{-1} correspond to C=C stretching vibrations from aromatic rings, all from plant metabolites. The stretching band at 1757 cm^{-1} could be assigned to C=O stretching of lactones, ketones, or carboxylic anhydrides. Other vibrations at 1514 and 1267 cm^{-1} are attributed to C=C of the aromatic ring and C–O groups stretching in phenol, ester, and ether, respectively. The peak at 1379 cm^{-1} corresponds to

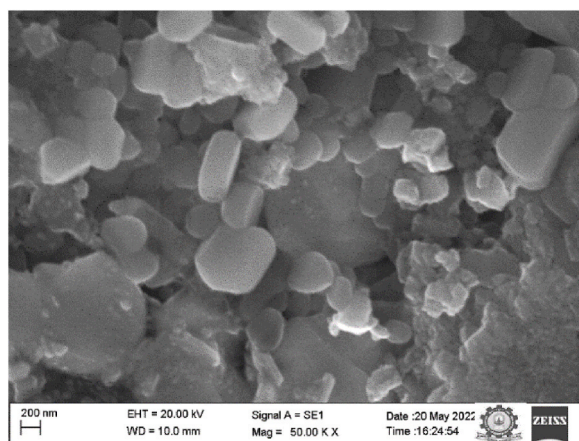


Fig. 6. Morphology of the Ag NPs.

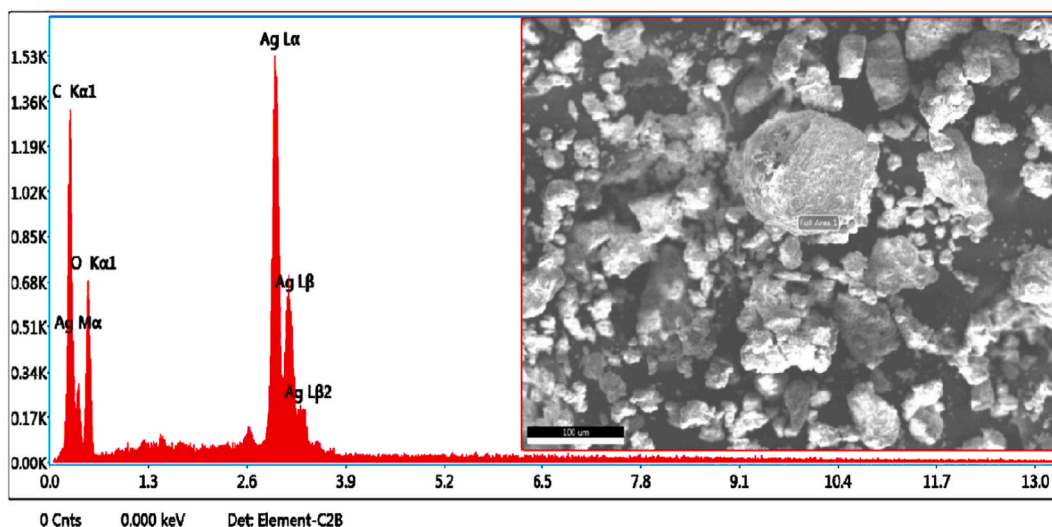


Fig. 7. Energy Dispersive X-Ray (EDX) spectrum of synthesized Ag NPs.

Table 2

(a) – Testing analysis for area 1.

Element	Weight (%)	Atomic (%)	Error (%)	K ratio
C K	19.2	39.7	6.0	0.1501
O K	31.5	49	12	0.0497
AgL	49.3	11.4	3.4	0.4293

(b) – Testing analysis for area 2

Element	Weight (%)	Atomic (%)	Error (%)	Kratio
C K	28.4	72.8	11.6	0.0446
O K	71.6	27.2	2.2	0.6615

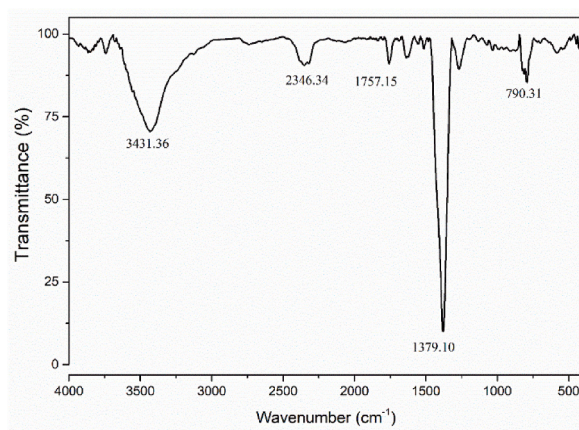


Fig. 8. FTIR spectra of synthesized Ag NPs.

the C–N stretching of the aromatic amine group. The peak at 790 cm^{-1} is attributed to aromatic groups. Ag NPs synthesized using Rosy Periwinkle leaf extract also contained a variety of functional groups, such as alkene, amine, and carboxylic acids. Most of these functional groups belong to major chemical groups classes; they have been shown to act as reducing agents in the synthesis of Ag NPs.

3.4. X-ray power diffusion analysis

Rosy Periwinkle leaf extract, Ag NPs were further demonstrated and confirmed by XRD analysis Fig. 9. In XRD analysis, the intensity

is estimated with respect to different angles, where it is observed that the peaks are identified at 38.12° , 44.31° , 64.41° , and 77.46° . The XRD patterns revealed that Ag NPs are reflected in the 2θ on 38.12° , 44.31° , 64.41° , and 77.46° , which correspond to the (111), (200), (220), and (311) Bragg reflections of the sample and which ensures that Ag NPs have crystalline structure. The bio synthesized Ag NPs, which is face-centered cubic (fcc) structure having JCPDS standard No. 87–3722. As a result, XRD patterns revealed that the Ag NPs formed by the lowering of Ag⁺ ions by AgNO₃ in the extract of the *Rosy Periwinkle* leaf.

It is concluded that the UV–visible spectrum of the solution containing Ag NPs showed an absorption peak at 408 nm. Ag NPs were shaped by the lowering of Ag⁺ ions by AgNO₃ in the extract of the *Rose Periwinkle* leaf, as shown by the XRD patterns. By using biomolecules that were identified in the FTIR spectrum of the leaf extract, Ag NPs were reduced and capping was achieved. Under Scanning Electron Microscope (SEM), the shape of the Ag NPs was mostly count to be in spherical shape and few particles were found to agglomerated in to larger particles with unclear morphology. Silver was present, as shown by the produced Ag NPs EDX pattern. Overall, a variety of characterization approaches were used to examine the environmentally friendly and less harmful manufactured product. As a result, Ag NPs were used as a coating for solar panels to increase efficiency.

3.5. Conductivity testing

The green synthesis process has advanced solar cell conductance in prevalent aspects. Ag NPs exhibited color changes because of the excitation of surface plasmon vibration within the particles. In this research work, the *Rosy Periwinkle* plant leaves are used to get the extract for producing Ag NPs in order to coat the solar panel, and this type of coating helps to increase the electrical conductivity due to photoelectric effect because of the presence of silver in solar panel. In order to determine the performance of the proposed model, the conductivity test is carried out in this work. During this analysis, the electric conductivity is validated for analyzing the presence of silver particles. The findings indicate that the conductivity of the solar panel has been determined as 0.300 ms/cm and the resistance of the solar is 3.33 Ω for conductance (G).

3.6. VI and PV characteristics analysis

In this study, the performance of the proposed green synthesis method is validated and tested according to the current density characteristics. As shown in Fig. 10, the parameter such as V_{oc} , I_{sc} , V_{mp} , I_{mp} and efficiency are validated and tested under changing irradiation conditions such as 1000 W/m², 500 W/m², and 200 W/m². Also, the suggested parameters are estimated for before and after panel coating with Ag NPs. At 1000 W/m² irradiance for a 3 W panel, $V_{oc} = 10.8$ V, $I_{sc} = 0.391$ A, V_{mp} , and I_{mp} are 9.72 V and 0.391 A at this instant, efficiency will be 17.20 % for a coated solar panel when compared to non-coated panel efficiency will be 14.77 %. In addition to that, the irradiance level of 500 W/m², and 200 W/m² efficiency will be increased from 15.42 % to 18 % and 16.76 % to 19.20 %. Table 2 demonstrates the various parameter variances and concludes the perfect radiance level for both coated and non-coated solar panels. The results indicate that the overall performance of the coated solar panel has been greatly improved, when compared to the typical solar panel (see Table 3).

This simulation setup of the silver-coated solar panel has simulated different kinds of load values. Figs. 11 and 12 reveals the VI and PV characteristics of 1000 W/m² irradiation. Typically, the power tracking efficiency of the solar panel has been determined according to the VI and PV characteristics. For this analysis, these parameters are estimated for both the coated and non-coated panels. The obtained results reveal that the current and power both are highly improved for the coated panel, when comparing it to the non-coated panel. Due to an effective coating with Ag NPs, the overall power tracking efficiency of the coated panel is increased with better VI and PV characteristics. The comparison graph illuminates that the performance of Ag NPs coated solar panels was better than the non-coated solar panel in 1000w/m².

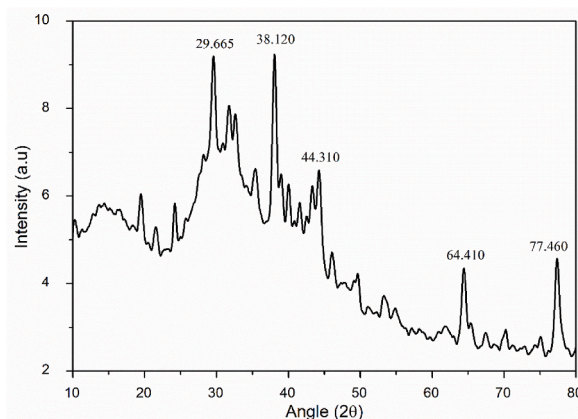


Fig. 9. X-ray diffractogram of the synthesized Ag NPs.

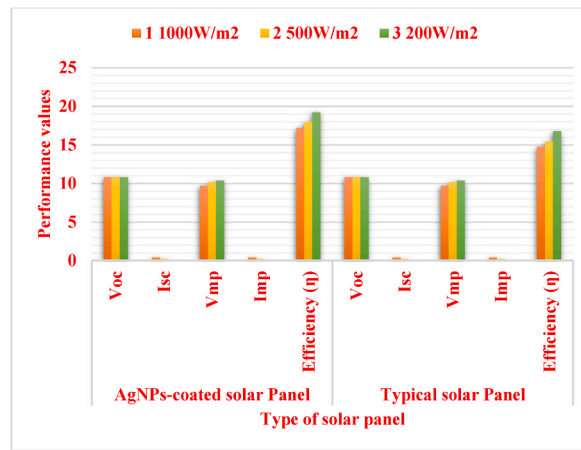


Fig. 10. Current density characteristics under simulation.

Table 3

Performance characteristics of Ag NPs coated and non-coated solar panels by simulation.

S. No	Irradiance level (W/m ²)	Ag NPs-coated solar Panel					Typical solar Panel				
		V _{oc}	I _{sc}	V _{mp}	I _{mp}	Efficiency (η)	V _{oc}	I _{sc}	V _{mp}	I _{mp}	Efficiency (η)
1.	1000	10.8	0.391	9.72	0.391	17.20	10.8	0.383	9.72	0.383	14.77
2.	500	10.8	0.1955	10.152	0.195	18.00	10.8	0.1915	10.152	0.191	15.42
3.	200	10.8	0.0782	10.368	0.0781	19.20	10.8	0.077	10.368	0.0765	16.76

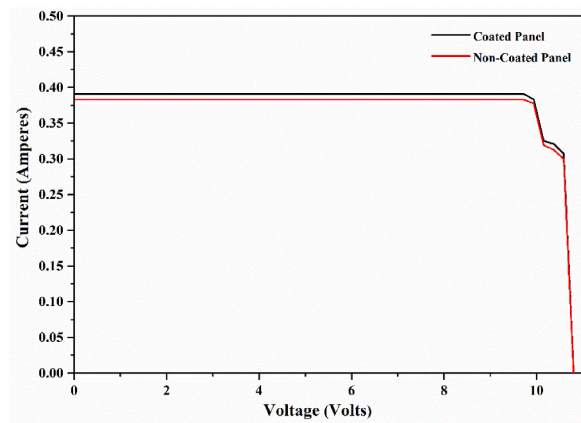


Fig. 11. VI characteristics of 1000 W/m² irradiation.

3.7. Experimental analysis

In this study, the experimental analysis is also carried out by testing the proposed model with the use of flash testers. Here, the output performance and conformity of the proposed scheme is validated and measured with the use of flash test machine, which is also known sun simulator. For this assessment, the evaluation parameters are validated with respect to different test conditions, in which the temperature, output voltage, and maximum power are the most crucial parameters used to analyze the system efficacy. The experimentation of the solar panel has correlated with the Ag NPs coating and non-coating solar panels. As shown in Table 4 and Fig. 13, the performance of the non-coated and coated solar panels with Ag NPs are validated and compared based on the parameters of V_{OC}, I_{SC}, V_{MP}, I_{MP}, and efficiency under changing irradiations.

A solar panel Maximum Power Point (MPP) is positioned near the bend in the VI characteristics curve. The corresponding values of V_{mp} and I_{mp} can be estimated from coated and non-coated solar panels of 3 W. The efficiency of a coated solar panel was 14 % whereas the efficiency of a non-coated panel was 11.8 % at 1000 W/m² irradiance for a 3 W panel, V_{oc} = 10.8 V, I_{sc} = 0.391 A, V_{mp} and I_{mp} are 9 V and 0.342 A at this moment. The increase in percentage of efficiency was 2.2 %. In addition to that, the irradiance level of 500 W/

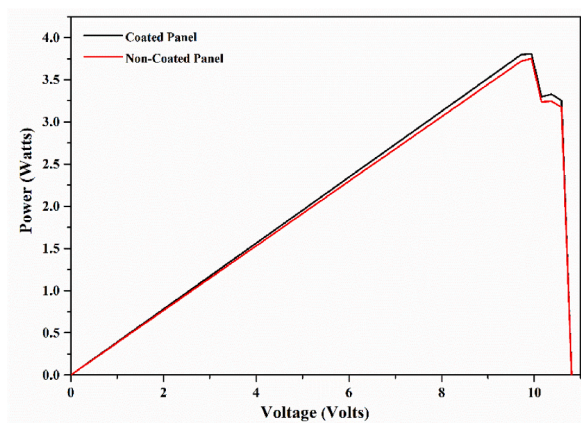


Fig. 12. PV characteristics of 1000 W/m² irradiation.

Table 4

Performance characteristics of Ag NPs coated and non-coated solar panels under a real-time environment.

S.No	Irradiance level (W/m ²)	Ag NPs-coated solar Panel					Typical solar Panel				
		V _{oc}	I _{sc}	V _{mp}	I _{mp}	Efficiency (η)	V _{oc}	I _{sc}	V _{mp}	I _{mp}	Efficiency (η)
1.	1000	10.8	0.391	9	0.342	14	10.8	0.383	9	0.333	11.8
2.	500	10.8	0.1924	10.052	0.191	14.8	10.8	0.1902	10.052	0.190	12.45
3.	200	10.8	0.0764	10.35	0.074	16.1	10.8	0.071	10.32	0.0745	13.79

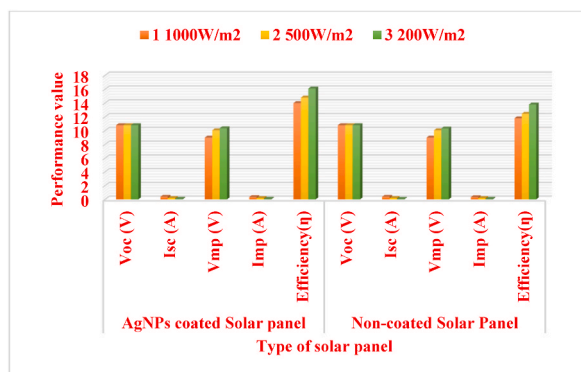


Fig. 13. Current density characteristics under real-time environment.

m², and 200 W/m² efficiency was increased from 12.45 % to 14.8 % and 13.79 %–16.1 %. The performance factors like efficiency were improved by the current density characteristics in a real-time environment. From the overall simulation as well as experimental results, it is analyzed that the performance outcomes of the coated solar panel are effectively improved in both assessments. Moreover, an effective green synthesis and characterization analyses support to get an increased efficiency, when comparing it to the non-coated solar panel.

The comparison graph of the solar panel has been computed in Fig. 14. The comparison graph of the coated and non-coated solar panels enlightens the performance of coated solar panel over the non-coated solar panel. When the maximum power voltage (V_{mp}) of the solar panel is 10.36 V, the maximum power current (I_{mp}) is 765 μA (before Ag NPs coating), and the maximum power current (I_{mp}) is 780 μA (after Ag NPs coating). The P–V characteristics curve of a solar panel before and after being coated with Ag NPs is shown in Fig. 15. While the maximum power voltage (V_{mp}) of the solar panel is 10.36 V, the maximum power (P_{mp}) is 0.6 W (before Ag NPs coating), and the maximum power (P_{mp}) is 0.82 W (after Ag NPs coating).

4. Conclusions

This paper implemented an effective green synthesis method for coating solar panels with the use of Ag NPs. The proposed study makes a novel contribution by coating the solar panels with Ag NPs using *Rosy Periwinkle* plant leaves. This helps to significantly

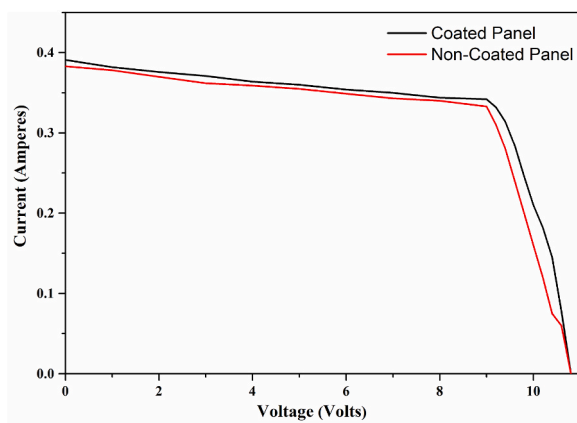


Fig. 14. VI characteristics of Solar Panel under experimental conditions.

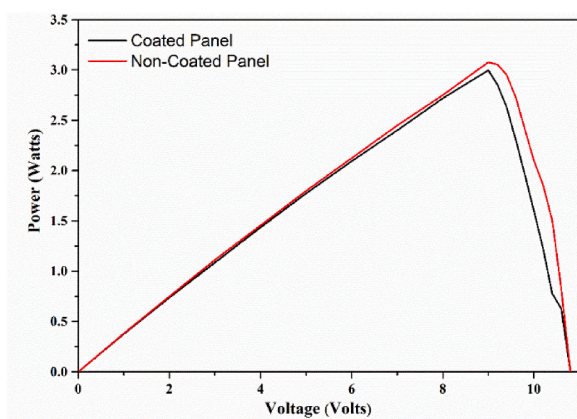


Fig. 15. PV characteristics of the coated and non-coated solar panel under experimental conditions.

increase in current characteristics with low-cost consumption. For this, Rosy Periwinkle plant leaves were gathered from the surrounding region of the study area, and its extract was obtained to generate Ag NPs. After this green synthesis, the characterization studies such as UV-Vis, SEM, EDX, FTIR, XRD, conductivity test and current density characteristics were carried out for an effective solar panel coating. Then, the panel is coated with the extracted Ag NPs on the c-si layer, which helps to improve the maximum tracking efficiency. Here, both the simulation study and experiment analysis are conducted for determining the overall solar panel efficiency before and after coating with Ag NPs. For simulation study, the MATLAB/Simulink tool is used to examine the VI and PV characteristics of the solar panel under changing irradiation conditions. For experimentation, the flash tester is used to test the solar panel efficiency under different irradiation condition. Moreover, the parameters such as V_{oc} , I_{sc} , V_{mp} , I_{mp} , and efficiency were validated and compared for both simulation and experimental analysis. According to the findings, it is determined that the coated solar panels with the Ag NPs provides improved performance results in terms of efficiency, and MPP. The results indicate that the efficiency was increased from 12.45 % to 14.8 % and 13.79 %–16.1 % under varying irradiance level of 500 W/m^2 , and 200 W/m^2 . By using the proper characterization and green synthesis operations, the overall efficiency of the solar panel coating method was improved. When comparing it to the non-coated panel. Since, a proper green synthesis, Ag NPs extraction, and characterization were the major reasons for an effective solar panel coating.

In future, the proposed work can be enhanced further by implementing this solar panel for smart-grid application system. Also, we have planned to use this PV panel for satisfying the energy demand of smart-grid systems with the advanced converter and controlling models.

CRedit authorship contribution statement

Priya Palanichamy: Conceptualization, Data curation, Methodology, Writing - original draft. **Rajesh Krishnasamy:** Conceptualization, Data curation, Formal analysis, Funding acquisition, Investigation, Project administration, Supervision, Validation, Writing - original draft, Writing - review & editing. **Ulaganathan Meenakshi Sundaram:** Conceptualization, Data curation, Formal analysis, Project administration, Validation, Writing - original draft. **Senthil Muthu Kumar Thiagamani:** Conceptualization, Data curation,

Investigation, Methodology, Supervision, Writing - original draft. **R.A. Ilyas:** Investigation, Project administration, Validation, Writing - original draft, Writing - review & editing. **Ahmed M. Hassan:** Funding acquisition, Project administration, Validation, Visualization, Writing - original draft, Writing - review & editing.

Declaration of competing interest

The authors declare that they have no known competing financial interests or personal relationships that could have appeared to influence the work reported in this paper.

Acknowledgement

The authors thank the management of Kalasalingam Academy of Research and Education for providing fabrication and testing facilities. The authors thank the faculty of engineering, Future University in Egypt for financial support.

References

- [1] S. Ahmad, S. Munir, N. Zeb, A. Ullah, B. Khan, J. Ali, et al., Green nanotechnology: a review on green synthesis of silver nanoparticles—an ecofriendly approach, *Int. J. Nanomed.* (2019) 5087–5107.
- [2] M.A. Huq, M. Ashrafudoulla, M.M. Rahman, S.R. Balusamy, S. Akter, Green synthesis and potential antibacterial applications of bioactive silver nanoparticles: a review, *Polymers* 14 (2022) 742.
- [3] M. Abbasi, R. Gholizadeh, S.R. Kasaei, A. Vaez, S. Chelliapan, F. Fadhil Al-Qaim, et al., An intriguing approach toward antibacterial activity of green synthesized Rutin-templated mesoporous silica nanoparticles decorated with nanosilver, *Sci. Rep.* 13 (2023) 5987.
- [4] F. Ghorbani, J. Shabanpour, S. Beyraghi, H. Soleimani, H. Oraizi, M. Soleimani, A deep learning approach for inverse design of the metasurface for dual-polarized waves, *Appl. Phys. A* 127 (2021) 1–7.
- [5] Y. Sadeghipour, M.H. Alipour, H.R. Ghaderi Jafarbigloo, A. Salahvarzi, M. Mirzaii, A.M. Amani, et al., Evaluation antibacterial activity of biosynthesized silver nanoparticles by using extract of *Euphorbia Pseudocactus* Berger (*Euphorbiaceae*), *Nanomed. Res. J.* 5 (2020) 265–275.
- [6] M.A.J. Rouhbanani, S. Mosleh-Shirazi, N. Beheshtkhoo, S.R. Kasaei, S. Nekouian, S. Alshehry, et al., Investigation through the antimicrobial activity of electrospun PCL nanofiber mats with green synthesized Ag–Fe nanoparticles, *J. Drug Deliv. Sci. Technol.* 85 (2023), 104541.
- [7] A.S. Jain, P.S. Pawar, A. Sarkar, V. Junnuthula, S. Dyawanapelly, Bionanofactories for green synthesis of silver nanoparticles: toward antimicrobial applications, *Int. J. Mol. Sci.* 22 (2021), 11993.
- [8] D. Garibo, H.A. Borbón-Núñez, J.N.D. de León, E. García Mendoza, I. Estrada, Y. Toledano-Magaña, et al., Green synthesis of silver nanoparticles using *Lysiloma acapulcensis* exhibit high-antimicrobial activity, *Sci. Rep.* 10 (2020), 12805.
- [9] A. Roy, O. Bulut, S. Some, A.K. Mandal, M.D. Yilmaz, Green synthesis of silver nanoparticles: biomolecule-nanoparticle organizations targeting antimicrobial activity, *RSC Adv.* 9 (2019) 2673–2702.
- [10] H. Yousof, A. Mehmood, K.S. Ahmad, M. Raffi, Green synthesis of silver nanoparticles and their applications as an alternative antibacterial and antioxidant agents, *Mater. Sci. Eng. C* 112 (2020), 110901.
- [11] N.S. Alharbi, N.S. Alsubhi, A.I. Felimban, Green synthesis of silver nanoparticles using medicinal plants: characterization and application, *J. Radiat. Res. Appl. Sci.* 15 (2022) 109–124.
- [12] F. Jalilian, A. Chahardoli, K. Sadrjavadi, A. Fattahi, Y. Shokoohinia, Green synthesized silver nanoparticle from *Allium ampeloprasum* aqueous extract: characterization, antioxidant activities, antibacterial and cytotoxicity effects, *Adv. Powder Technol.* 31 (2020) 1323–1332.
- [13] A. Bouafia, S.E. Laouini, A.S. Ahmed, A.V. Soldatov, H. Algarni, K. Feng Chong, et al., The recent progress on silver nanoparticles: synthesis and electronic applications, *Nanomaterials* 11 (2021) 2318.
- [14] D.K. Poudel, P. Niraula, H. Aryal, B. Budhathoki, S. Phuyal, R. Marahatha, et al., Plant-mediated green synthesis of Ag NPs and their possible applications: a critical review, *J. Nanotechnol.* 2022 (2022).
- [15] L. Castillo-Henriquez, K. Alfaro-Aguilar, J. Ugalde-Álvarez, L. Vega-Fernández, G. Montes de Oca-Vásquez, J.R. Vega-Baudrit, Green synthesis of gold and silver nanoparticles from plant extracts and their possible applications as antimicrobial agents in the agricultural area, *Nanomaterials* 10 (2020) 1763.
- [16] B. Singh, M.M. Shabat, D.M. Schaadt, Silver nanoparticle-based anti-reflection coating for solar cells, *Photon. Solar Energy Syst.* VIII (2020) 59–64.
- [17] D. Chugh, V. Viswamalya, B. Das, Green synthesis of silver nanoparticles with algae and the importance of capping agents in the process, *J. Genet. Eng. Biotechnol.* 19 (2021) 1–21.
- [18] A.A. Tabrizi, A. Pahlavan, Efficiency improvement of a silicon-based thin-film solar cell using plasmonic silver nanoparticles and an antireflective layer, *Opt Commun.* 454 (2020), 124437.
- [19] H. Ye, X. Li, L. Deng, P. Li, T. Zhang, X. Wang, et al., Silver nanoparticle-enabled photothermal nanofibrous membrane for light-driven membrane distillation, *Ind. Eng. Chem. Res.* 58 (2019) 3269–3281.
- [20] R. Shashanka, H. Esgin, V.M. Yilmaz, Y. Caglar, Fabrication and characterization of green synthesized ZnO nanoparticle based dye-sensitized solar cells, *J. Sci.: Adv. Mater. Dev.* 5 (2020) 185–191.
- [21] P. Pattanayak, P. Behera, D. Das, S.K. Panda, *Ocimum sanctum* Linn. A reservoir plant for therapeutic applications: an overview, *Phcog. Rev.* 4 (2010) 95.
- [22] B.S. Kendler, Garlic (*Allium sativum*) and onion (*Allium cepa*): a review of their relationship to cardiovascular disease, *Prev. Med.* 16 (1987) 670–685.
- [23] S. Gajalakshmi, S. Vijayalakshmi, R.V. Devi, Pharmacological activities of *Catharanthus roseus*: a perspective review, *Int. J. Pharma Bio Sci.* 4 (2013) 431–439.